

# 靶增强正交双脉冲激光诱导击穿光谱的信号增强机制研究

林泽浩, 李润华, 姜银花, 陈钰琦\*

华南理工大学物理与光电学院, 广东 广州 510641

**摘要** 为了更好地解决正交双脉冲激光诱导击穿光谱(DP-LIBS)技术中再加热激光能量利用率低、信号增强效果不理想的难题,本研究团队建立了靶增强正交 DP-LIBS 技术,并研究了其信号增强机理。将再加热激光作用于铝靶表面产生靶等离子体,通过靶等离子体与样品等离子体的相互作用来显著增强样品元素的信号强度。以黄铜为样品,本团队通过实验研究了脉冲延时对原子辐射强度的影响,并分析了等离子体温度变化和光学辐射的时域演化特性。研究表明:在优化的实验条件下,靶增强技术可以在传统再加热正交 DP-LIBS 的基础上,使样品元素的信号强度继续显著增强。信号增强主要来自等离子体温度的升高和碰撞机制。该技术能显著增强正交 DP-LIBS 的信号强度,对于进一步提高正交 DP-LIBS 的光谱分析灵敏度、取得更理想的分析效果具有较重要的科学意义。

**关键词** 光谱学; 激光诱导击穿光谱; 激光等离子体; 正交双脉冲; 固体靶; 信号增强

中图分类号 O433.5

文献标志码 A

doi: 10.3788/CJL202148.2411001

## 1 引言

正交双脉冲激光诱导击穿光谱(DP-LIBS)技术是一种极具潜力的微烧蚀高灵敏元素分析技术。基于双脉冲的相对延时,正交 DP-LIBS 技术可分为预烧蚀和再加热两种类型<sup>[1]</sup>。在元素分析过程中,再加热正交 DP-LIBS 技术可以在保留单脉冲 LIBS 快速分析、微烧蚀以及多元素同时分析等优点的前提下增强光谱强度<sup>[2-5]</sup>,同时还具有受自吸收效应影响小且剥离所需激光能量低的优点<sup>[6-8]</sup>,非常适合用于贵重样品或少量样品的微烧蚀元素分析以及高空间分辨的元素分布成像分析<sup>[9-12]</sup>。为了方便叙述,如果没有特别说明,后文所有正交 DP-LIBS 均指再加热正交 DP-LIBS。

正交 DP-LIBS 技术也存在不足之处。首先,在正交 DP-LIBS 中,第二路的再加热激光作用于第一路激光产生的等离子体上,样品只能吸收一部分激光能量,使得激光的能量利用率低;其次,由于等离子体的粒子密度低,且没有引入额外的碰撞来增强

信号,因此在开展定量分析时,与单脉冲 LIBS 相比,正交 DP-LIBS 对元素检出限的改善效果并不太理想。余洋等<sup>[13]</sup>采用正交 DP-LIBS 技术对含铬土壤样品进行了分析,结果表明,其元素检出限的改善因子约为单脉冲 LIBS 技术的 2 倍;Wang 等<sup>[14]</sup>采用正交 DP-LIBS 技术分析了合金钢中的微量元素,结果表明,元素检出限的改善因子为 1.81~3.46;王金梅课题组<sup>[15]</sup>采用正交 DP-LIBS 分析了黄连中的微量元素,结果发现,铜和铅元素检出限的改善因子分别为 2.69 和 3.59。

近年来,为了进一步提高正交 DP-LIBS 技术的检测能力,大部分研究工作主要集中在增强等离子体光谱辐射强度和信号增强因子上,以获得更好的光谱分析效果。Bai 等<sup>[16]</sup>通过共心腔的多次反射对再加热激光进行了重复利用,结果发现,光谱信号增强因子可以达到原正交 DP-LIBS 技术的 2.3~3.6 倍;Prochazka 等<sup>[17]</sup>采用正交三脉冲 LIBS 技术将预烧蚀和再加热 DP-LIBS 技术融合在一起,该技术的信背比比 DP-LIBS 技术增强了 5 倍;但是这

收稿日期: 2021-04-14; 修回日期: 2021-05-13; 录用日期: 2021-05-24

基金项目: 国家自然科学基金(61875055)

通信作者: \*chenyuqi@scut.edu.cn

种正交三脉冲 LIBS 技术需要三路激光,增加了系统的复杂度。

为了更好地解决正交 DP-LIBS 中再加热激光能量利用率低、信号增强效果不理想的问题,本课题组提出了靶增强正交 DP-LIBS 技术,并研究了其信号增强机理。该技术将再加热激光聚焦在固体靶表面产生高温靶等离子体,通过靶等离子体与样品等离子体的相互作用来显著增强样品元素的信号强度。本课题组以黄铜为样品,通过实验研究了脉冲延时对原子辐射强度的影响,测定了等离子体温度和光学辐射的时域演化特性,并对靶增强正交 DP-LIBS 技术信号的增强机理进行了讨论。

## 2 实验装置

图 1 是实验装置示意图。采用一台中心波长为 1064 nm 的电光调 Q Nd:YAG 激光器作为等离子体激发光源,激光通过焦距为 60 mm 的聚焦透镜 L1 会聚在样品表面,对样品进行剥离并形成等离子

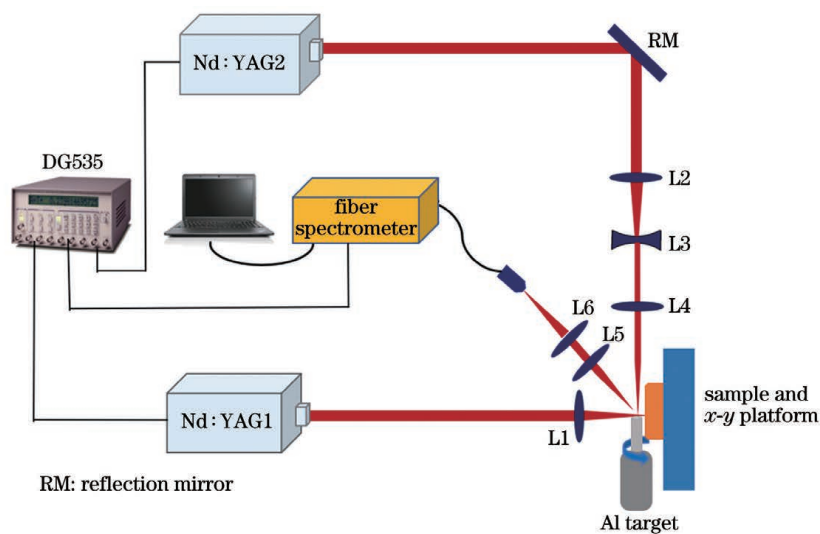


图 1 实验装置图

Fig. 1 Diagram of the experimental setup

等离子体辐射通过石英透镜 L5 ( $f=150\text{ mm}$ ) 收集并准直,最后被石英透镜 L6 ( $f=100\text{ mm}$ ) 聚焦到多通道光谱仪 (AvaSpec-ULS2048-3-USB2 型) 的光纤入口, DG535 同时为光纤光谱仪提供同步触发信号。该多通道光谱仪能够分析 200~550 nm 波长范围内的光谱。CCD 探测器具有 2048 像素,光谱分辨率优于 0.15 nm。为了对等离子体发射进行时域观测,本研究团队还利用 WDS-5 型单色仪和 CR114 型光电倍增管进行了探测,并采用 GDS-3502 型数字存储示波器监测光电倍增管的输出信号。

体。四通道数字延时脉冲发生器 (DG535 型) 用于触发并控制两激光光束的相对延时。另一台中心波长为 1064 nm 的电光调 Q Nd:YAG 激光器输出的激光通过凸透镜 L2 ( $f=250\text{ mm}$ ) 和凹透镜 L3 ( $f=-100\text{ mm}$ ) 组成的缩束系统后,由焦距为 80 mm 的聚焦透镜 L4 垂直聚焦于铝靶表面,对铝靶进行烧蚀形成铝等离子体。这两台电光调 Q Nd:YAG 激光器的脉宽均为 12 ns,工作重复频率均设定为 5 Hz。直径为 6 mm 的纯铝靶水平靠近样品表面,并在一直流电机的带动下匀速旋转,以避免激光长时间作用于一点而对铝靶造成过度烧蚀。这里应使两路激光形成的等离子体在空间位置上尽可能重合,同时应确保第二束激光所形成的等离子体不会单独剥离样品并激发出相应的原子辐射。相较于传统 DP-LIBS,靶增强 DP-LIBS 中的第二束激光焦点与样品表面的最佳距离略有不同,可以通过观察双脉冲激发条件下的原子辐射信号来确定。

本实验采用的样品为黄铜标准样品,样品中 Cu、Zn、Bi、Fe、Sn 元素的质量分数分别为 60.140%、33.293%、0.826%、0.645%、2.007%。样品安装在二维运动平台上并与平台一起作匀速运动,以保证激光的每一个脉冲都打在样品的不同位置上,从而保证了产生的等离子体的稳定性,也有助于得到均匀可靠的光谱。

## 3 分析与讨论

### 3.1 时间分辨光谱和脉冲延时的优化

图 2 显示了在 DP-LIBS 和靶增强条件下,利用

单色仪和光电倍增管在 324.75 nm 和 324.00 nm 波长处记录到的等离子体发射光谱信号时域图。其中第一束激光能量为 5 mJ, 第二束激光能量为 25 mJ, 两路激光脉冲延时为 4.0  $\mu\text{s}$ 。324.75 nm 的谱线对应 Cu 原子谱线。从图 2 中可以看出: 在正交 DP-LIBS 技术中, Cu 原子辐射信号的维持时间约为 12.0  $\mu\text{s}$ ; 采用靶增强技术后, Cu 原子辐射信号的维持时间延长至 18.0  $\mu\text{s}$ , 而此时对应于 324.00 nm 处的背景辐射的维持时间短于 1.5  $\mu\text{s}$ , 因而其时间积分强度显著增强, 这将有利于时间分辨的信号检测。如果将信号采集门选为 6.5~18.0  $\mu\text{s}$ , 则在当前实验条件下, 靶增强后的 Cu 原子辐射的时间积分强度可以获得约 7 倍的提高(与正交 DP-LIBS 技术相比)。

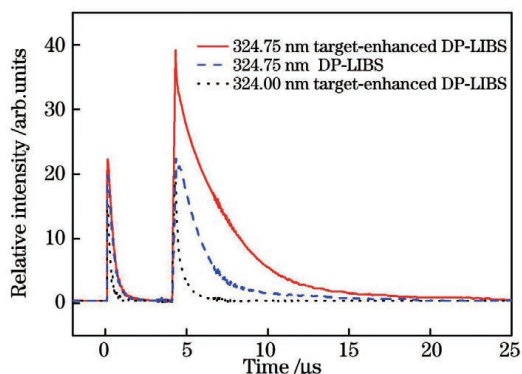


图 2 黄铜样品等离子体辐射的时域图

Fig. 2 Temporal profiles of plasma emission of brass sample

在靶增强正交 DP-LIBS 技术中, 第一束脉冲激光对样品进行烧蚀形成样品等离子体, 在样品等离子体膨胀、冷却过程中, 利用再加热激光对正交配置的金属铝靶进行烧蚀形成高温靶等离子体, 靶等离子体与样品等离子体相互作用, 可以显著增强样品元素的光学辐射。为了获得最佳的激发效率, 需要选取合适的激光光束相对延时。本研究团队以 Cu 原子辐射在 324.75 nm 处的特征谱线作为分析对象, 得到了两束激光脉冲相对延时在 0~30  $\mu\text{s}$  时间范围内时, Cu 原子辐射信号强度随激光脉冲相对延时的变化, 如图 3 所示。图 3 表明, 随着激光脉冲相对延时的增加, 光谱强度呈现出先增强后减弱的趋势。再加热激光聚焦至铝靶表面形成高温等离子体并与样品等离子体相互作用, 使等离子体内部的粒子数增加, 粒子间碰撞加剧。当作用时间不同时, 粒子相互碰撞效率、等离子体演化特性以及向外辐射的光谱特性也将不同。因此, 当激光光束相对延时

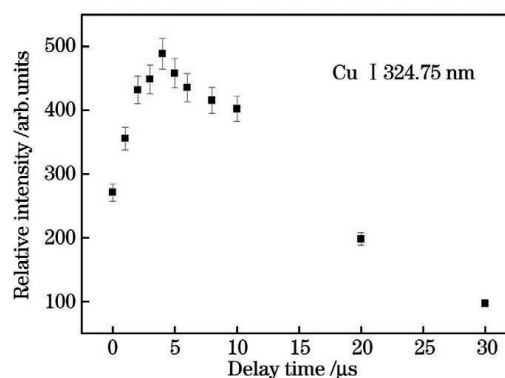


图 3 靶增强正交 DP-LIBS 中 Cu 原子分析线 324.75 nm 辐射光谱强度随激光光束相对延时的变化

Fig. 3 Plot of signal intensity of Cu I 324.75 nm in target-enhanced orthogonal DP-LIBS versus delay time between two pulses

较小时, 铝靶等离子体不能与样品等离子体充分作用, 而当激光光束相对延时过大时, 样品等离子体已膨胀飞出, 无法达到增强的效果。在当前实验条件下(第一束激光能量为 5 mJ, 第二束激光能量为 25 mJ), 综合考虑光谱强度和信号背景, 选择最佳激光光束相对延时约为 4.0  $\mu\text{s}$ 。

### 3.2 光谱强度增强

固定激光光束相对延时为 4.0  $\mu\text{s}$ , 利用紧凑型 Avantes 光纤光谱仪观测了单脉冲 LIBS (SP-LIBS)、正交 DP-LIBS 和靶增强正交 DP-LIBS 条件下黄铜样品的等离子体辐射光谱。图 4 为 323.00~331.00 nm 波长范围内所记录的等离子体辐射光谱。光纤光谱仪的采样门宽为 1.5 ms, SP-LIBS 和正交 DP-LIBS 探测时的积分延时分别为 1.5  $\mu\text{s}$  和 5.5  $\mu\text{s}$ 。图 4 下部为 SP-LIBS 条件下的光谱, 上部为正交 DP-LIBS 和靶增强正交 DP-LIBS 条件下的

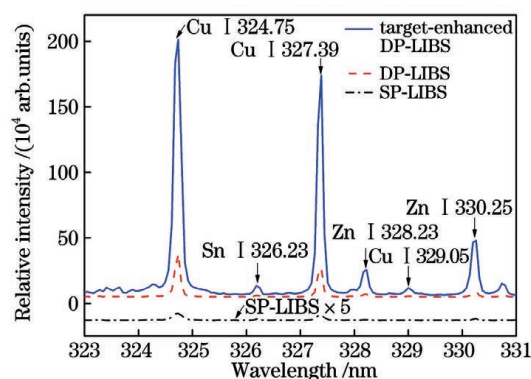


图 4 SP-LIBS、正交 DP-LIBS 和靶增强 DP-LIBS 条件下的等离子体发射谱

Fig. 4 Emission spectra of plasma in SP-LIBS, orthogonal DP-LIBS, and target-enhanced orthogonal DP-LIBS

光谱。由图 4 可以看出:SP-LIBS 条件下的等离子体辐射信号非常微弱;相较于 SP-LIBS,采用正交 DP-LIBS 时,Cu I 324.75 nm 分析线的信号增强了约 14 倍;增加铝靶后,Cu I 324.75 nm 分析线的信号增强了约 114 倍。

表 1 给出了相较于 SP-LIBS 和正交 DP-LIBS,黄铜标样中不同元素分析线信号强度在靶增强条件下的信号增强因子。由表 1 可见,靶增强技术可以在传统正交 DP-LIBS 的基础上,使样品元素的信号强度显著提高。传统正交 DP-LIBS 技术中再加热激光直接作用于样品等离子体,等离子体的粒子数密度较低,再加热激光的能量没有完全被样品等离子体吸收,导致再加热激光脉冲的能量利用率较低。采用靶增强技术后,由于固体铝靶的密度远高于气态等离子体的密度,在靶表面产生了高温且粒子密度相对较大的激光等离子体,向样品等离子体中注入了更多粒子,由于升温和碰撞等因素,等离子体中样品元素的信号强度得以有效增强。由于采用正交的几何空间配置,再加热激光并不直接剥离样品,因此相较于传统的正交 DP-LIBS 技术,靶增强 DP-LIBS 技术有助于在相同的样品损伤条件下获得更高的检测灵敏度。

表 1 采用靶增强正交 DP-LIBS 时不同元素等离子体辐射信号强度的增强因子

Table 1 Enhancement factor of plasma emission intensity obtained in target-enhanced orthogonal DP-LIBS

Analytical line	Enhancement factor	
	Compared with SP-LIBS	Compared with orthogonal DP-LIBS
Bi I 306.77 nm	44.0	6.3
Cu I 324.75 nm	114.0	6.0
Sn I 317.5 nm	24.0	6.9
Zn I 334.50 nm	146.0	10.4
Fe I 404.58 nm	128.0	7.9

### 3.3 等离子体温度的确定

为了更好地了解靶增强正交 DP-LIBS 中光谱信号增强的物理机制,本团队利用 Boltzmann 图的方法对等离子体温度进行了计算。在正交 DP-LIBS 和靶增强正交 DP-LIBS 条件下,根据光纤光谱仪测得的离子体光谱,选择表 2 中所示的 5 条 Cu I 非共振线,利用 Boltzmann 平面作图(如图 5 所示),并基于拟合线的斜率计算了相应的等离子体温度<sup>[18]</sup>。光纤光谱仪的采样门宽为 1.5 ms,计算得到

的等离子体温度可以看作是在等离子体辐射持续时间内平均温度。在正交 DP-LIBS 条件下计算出的等离子体温度( $T_e$ )为 6874 K,采用靶增强后等离子体温度提高至 9752 K,提高了 2878 K。这说明在增加铝靶后,高温靶等离子体对样品等离子体的升温和碰撞作用显著提高了等离子体温度,从而增强了样品元素的信号强度。

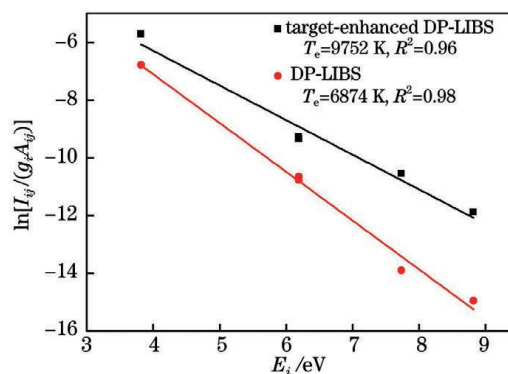


图 5 黄铜样品中 Cu 元素的 Boltzmann 平面

Fig. 5 Boltzmann plots of copper element for brass copper sample

表 2 用于计算等离子体温度的 Cu 原子谱线参数

Table 2 Spectroscopic parameters of copper atomic lines for plasma temperature calculation

Wavelength $\lambda$ /nm	Transition probability $A_{ij} / (10^8 \text{ s}^{-1})$	Degeneracy of the upper level $g_i$	Energy of the upper level $E_i$ /eV
330.79 (Cu I)	1.38	12	8.82
465.11 (Cu I)	0.38	8	7.74
510.55 (Cu I)	0.02	4	3.82
515.32 (Cu I)	0.60	4	6.19
521.82 (Cu I)	0.75	6	6.19

### 3.4 等离子体电子密度的讨论

对于通常的 LIBS 分析而言,谱线的展宽主要来自 Stark 展宽,Stark 效应所导致的谱线展宽与电子密度成正比<sup>[19]</sup>。对于等离子体谱线的展宽,通常只考虑 Stark 展宽和仪器展宽,Doppler 展宽、共振展宽、自然展宽的影响在估算时可以忽略不计,因此谱线的 Stark 展宽可以近似表示为实验观察到的谱线展宽减去仪器展宽。通过测量低压汞灯的光谱,得到本实验中所用光纤光谱仪的仪器展宽为 0.11 nm。这里选取 Cu I 324.75 nm 谱线进行洛伦兹拟合,估算 Stark 展宽,期望根据所选原子发射线的 Stark 展宽研究正交 DP-LIBS 和靶增强正交 DP-

LIBS 条件下平均电子密度的差异。Cu I 324.75 nm 谱线的洛伦兹拟合结果如图 6 所示,从图中可以看出,在正交 DP-LIBS 和靶增强正交 DP-LIBS 条件下,谱线的 Stark 展宽没有明显区别。因此,在目前

的实验条件下无法分辨出所选原子发射线的 Stark 展宽的差别。分析认为,虽然增加铝靶后在等离子体中注入了更多的粒子,增加了粒子间的碰撞,但电子密度的变化可能并不明显。

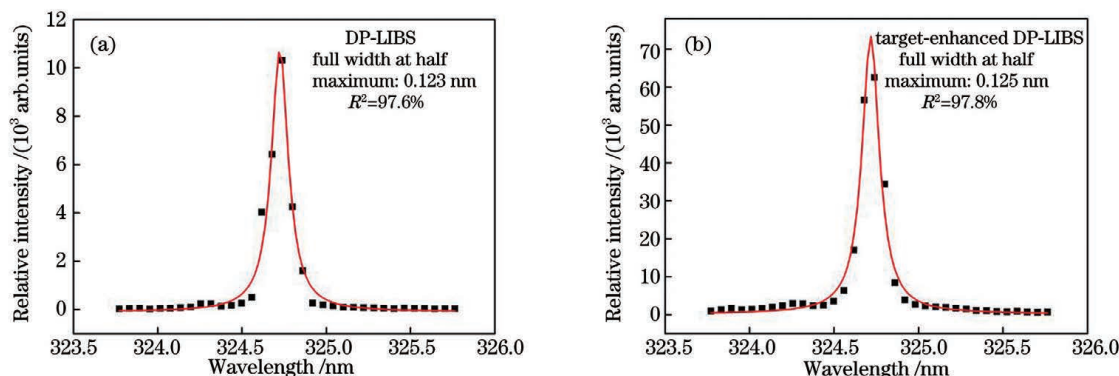


图 6 Cu 元素 324.75 nm 特征谱线的洛伦兹拟合图。(a)正交 DP-LIBS;(b)靶增强正交 DP-LIBS

Fig. 6 Lorentz fitting diagrams of Cu at 324.75 nm spectral line. (a) Orthogonal DP-LIBS; (b) target-enhanced orthogonal DP-LIBS

值得说明的是,在不增加剥离激光能量的情况下,采用金属铝靶与再加热激光作用产生高温靶等离子体,在高温靶等离子体与样品等离子体的相互作用下,传统正交 DP-LIBS 的信号增强因子可以得到显著改善。金属铝靶的加入可以减少样品损耗,同时方便开展高灵敏度的元素分析,特别适用于贵重样品和少量样品的微烧蚀元素分析。下一步,本团队将选取和研究其他谱线干扰少的金属和非金属固体靶材,期望能获得更好的信号增强效果。

## 4 结 论

本文提出了一种可用于再加热正交 DP-LIBS 的信号增强方法,即:引入铝靶与再加热激光相互作用产生高温靶等离子体,通过高温靶等离子体与第一束激光产生的样品等离子体相互作用来显著增强样品元素的信号强度。该方法不仅提高了再加热激光能量的利用率和等离子体温度,还引入了额外的碰撞机制,使样品元素的信号获得显著增强。研究表明:靶增强正交 DP-LIBS 技术可以显著增强传统的再加热正交 DP-LIBS 技术的信号强度,改善其光谱分析灵敏度,这对于提高再加热正交 DP-LIBS 的光谱分析能力,进一步拓展其应用领域具有重要的科学意义。

## 参 考 文 献

- [1] Safi A, Bahreini M, Tavassoli S H. Comparative study of two methods of orthogonal double-pulse laser-induced breakdown spectroscopy of aluminum [J]. Optics and Spectroscopy, 2016, 120(3): 367-378.
- [2] Wang J M, Zheng H J, Zheng P C, et al. Spectral characteristics of coptis chinensis plasma induced by orthogonalre-heating double-pulse laser [J]. Chinese Journal of Lasers, 2018, 45(7): 0702006.  
王金梅, 郑慧娟, 郑培超, 等. 正交再加热双脉冲激光诱导黄连等离子体的光谱特性 [J]. 中国激光, 2018, 45(7): 0702006.
- [3] Rashid B, Ahmed R, Ali R, et al. A comparative study of single and double pulse of laser induced breakdown spectroscopy of silver [J]. Physics of Plasmas, 2011, 18(7): 073301.
- [4] Ahmed R, Baig M A. A comparative study of enhanced emission in double pulse laser induced breakdown spectroscopy [J]. Optics & Laser Technology, 2015, 65: 113-118.
- [5] Li W P, Zhou W D. Comparative study of underwater single pulse and orthogonal double pulse laser-induced breakdown spectroscopy of barium element in solution [J]. Chinese Journal of Lasers, 2019, 46(9): 0911003.  
李文平, 周卫东. 溶液中 Ba 元素的水下单脉冲与正交双脉冲 LIBS 的比较研究 [J]. 中国激光, 2019, 46(9): 0911003.
- [6] Santagata A, de Bonis A, Villani P, et al. Fs/ns-dual-pulse orthogonal geometry plasma plume reheating for copper-based-alloys analysis [J]. Applied Surface Science, 2006, 252(13): 4685-4690.
- [7] Contreras V, Meneses-Nava M A, Barbosa-García O, et al. Double-pulse and calibration-free laser-induced breakdown spectroscopy at low-ablative

- energies[J]. Optics Letters, 2012, 37(22): 4591-4593.
- [8] Suliyanti M M, Hidayah A N, Pardede M, et al. Double pulse spectrochemical analysis using orthogonal geometry with very low ablation energy and He ambient gas[J]. Spectrochimica Acta Part B: Atomic Spectroscopy, 2012, 69: 56-60.
- [9] Mo J Y, Chen Y Q, Li R H. Silver jewelry microanalysis with dual-pulse laser-induced breakdown spectroscopy: 266+1064 nm wavelength combination [J]. Applied Optics, 2014, 53(31): 7516-7522.
- [10] Lu Y, Zorba V, Mao X L, et al. UV fs-ns double-pulse laser induced breakdown spectroscopy for high spatial resolution chemical analysis [J]. Journal of Analytical Atomic Spectrometry, 2013, 28(5): 743-748.
- [11] Krajcarová L, Novotný K, Kummerová M, et al. Mapping of the spatial distribution of silver nanoparticles in root tissues of *Vicia faba* by laser-induced breakdown spectroscopy (LIBS)[J]. Talanta, 2017, 173: 28-35.
- [12] Klus J, Mikysek P, Prochazka D, et al. Multivariate approach to the chemical mapping of uranium in sandstone-hosted uranium ores analyzed using double pulse laser-induced breakdown spectroscopy[J]. Spectrochimica Acta Part B: Atomic Spectroscopy, 2016, 123: 143-149.
- [13] Yu Y, Zhao N J, Fang L, et al. Comparative study on laser induced breakdown spectroscopy based on single pulse and re-heating orthogonal dual pulse[J]. Spectroscopy and Spectral Analysis, 2017, 37(2): 588-593.  
余洋, 赵南京, 方丽, 等. 单脉冲和再加热正交双脉冲激光诱导击穿光谱对比研究[J]. 光谱学与光谱分析, 2017, 37(2): 588-593.
- [14] Wang J G, Li X Z, Li H H, et al. Analysis of the trace elements in micro-alloy steel by reheating double-pulse laser-induced breakdown spectroscopy [J]. Applied Physics B, 2017, 123(4): 1-7.
- [15] Zheng P C, Li X J, Wang J M, et al. Quantitative analysis of Cu and Pb in *Coptidis* by reheated double pulse laser induced breakdown spectroscopy[J]. Acta Physica Sinica, 2019, 68(12): 125202.  
郑培超, 李晓娟, 王金梅, 等. 再加热双脉冲激光诱导击穿光谱技术对黄连中 Cu 和 Pb 的定量分析[J]. 物理学报, 2019, 68(12): 125202.
- [16] Bai Y, Zhang L, Hou J J, et al. Concentric multipass cell enhanced double-pulse laser-induced breakdown spectroscopy for sensitive elemental analysis[J]. Spectrochimica Acta Part B: Atomic Spectroscopy, 2020, 168: 105851.
- [17] Prochazka D, Pořizka P, Novotný J, et al. Triple-pulse LIBS: laser-induced breakdown spectroscopy signal enhancement by combination of pre-ablation and re-heating laser pulses[J]. Journal of Analytical Atomic Spectrometry, 2020, 35(2): 293-300.
- [18] Gao J K, Kang J, Li R H, et al. Application of calibration-free high repetition rate laser-ablation spark-induced breakdown spectroscopy for the quantitative elemental analysis of a silver alloy [J]. Applied Optics, 2020, 59(13): 4091-4096.
- [19] Colón C, Hatem G, Verdugo E, et al. Measurement of the Stark broadening and shift parameters for several ultraviolet lines of singly ionized aluminum [J]. Journal of Applied Physics, 1993, 73(10): 4752-4758.

## Signal Enhancement in Target-Enhanced Orthogonal Double-Pulse Laser-Induced Breakdown Spectroscopy

Lin Zehao, Li Runhua, Jiang Yinhua, Chen Yuqi\*

School of Physics and Optoelectronics, South China University of Technology, Guangzhou, Guangdong 510641, China

### Abstract

**Objective** Orthogonal double-pulse (DP) laser-induced breakdown spectroscopy (LIBS) in reheating mode provides intrinsic advantages, such as reduced self-absorption, capability of quantitative elemental analysis using very low ablative laser pulse energy, and relatively large signal enhancement factor under low ablative laser pulse energy. Conventional reheating orthogonal DP-LIBS allows realizing sensitive elemental analysis under microablation or elemental mapping analysis with high spatial resolution. However, as the reheating laser is focused on sample plasma with low particle density, only part of the reheating laser can be absorbed, reducing the utilization efficiency of laser energy. Therefore, under high ablative laser pulse energy, the signal of orthogonal DP-LIBS cannot be suitably

enhanced compared with single-pulse LIBS using the same ablation laser. To improve the energy utilization efficiency in reheating laser and increase the signal enhancement factor in orthogonal DP-LIBS, target-enhanced orthogonal DP-LIBS is proposed, and its signal enhancement mechanism is studied.

**Methods** A solid target with low spectral interference was added in reheating orthogonal DP-LIBS. In addition, a rotating solid aluminum target was placed perpendicular to the target sample. Two electro-optically  $Q$ -switched Nd : YAG lasers with 5 Hz pulse repetition rate and 1064 nm wavelength were used as excitation sources. The beam of the first laser was perpendicularly focused on the sample surface to produce sample plasma, and the beam of the second laser was focused on the surface of the aluminum target to produce target plasma. Moreover, the focal spot of the second laser beam was located in front of the sample surface, and the distance from the focal spot to the sample surface was adjusted to avoid sample ablation by the second laser. For evaluation, a compact fiber-optic spectrometer coupled with a nonintensified charge-coupled device was used to record the spectra. In addition, a monochromator and a photomultiplier tube were used to record the temporal profile of the light emission, and a brass standard sample was analyzed.

**Results and Discussions** The signal intensities of the sample elements were significantly enhanced by the interaction between the target and sample plasmas. The temporal profiles of plasma emission from the brass sample were recorded at 324.75 and 324.00 nm using orthogonal DP-LIBS and the proposed target-enhanced orthogonal DP-LIBS. The persistence time of the copper atomic emission observed at 324.75 nm was prolonged to 18.0  $\mu\text{s}$  using the target-enhanced orthogonal DP-LIBS (Fig. 2). The effect of the interpulse delay on the atomic emission intensities was experimentally determined. The best delay time for the two laser pulses was approximately 4.0  $\mu\text{s}$ . In the target-enhanced orthogonal DP-LIBS, multiple emission lines of different elements could be simultaneously enhanced (Fig. 3). Under the optimal experimental conditions, the signal intensity was enhanced by a factor of 24–146 compared with single-pulse LIBS and by a factor of 6–10 compared with conventional orthogonal DP-LIBS. Thus, a substantial improvement in the intensity was obtained from aluminum target enhancement (Table 1). To clarify the signal enhancement mechanism of target enhancement, the plasma temperature variations in orthogonal DP-LIBS and target-enhanced orthogonal DP-LIBS were determined based on Boltzmann plots using various copper atomic lines. Plasma temperature was 6874 and 9752 K for orthogonal DP-LIBS and target-enhanced orthogonal DP-LIBS, respectively (Fig. 5), corresponding to a temperature increase of 2878 K. The averaged electron density in orthogonal DP-LIBS and the target-enhanced orthogonal DP-LIBS was evaluated according to the Stark broadening of selected atomic emission lines. Under the considered experimental conditions, the difference in Stark broadening of the selected atomic emission lines could not be distinguished. This may be owing to the change in electron density being negligible in both cases. Overall, the experimental results indicated that the proposed reheating target-enhanced orthogonal DP-LIBS could improve the signal for a given sample ablation condition compared with the conventional orthogonal DP-LIBS.

**Conclusions** A target-enhanced orthogonal DP-LIBS technique considering reheating is proposed. Using a solid target in conventional orthogonal DP-LIBS, plasma emission can be substantially enhanced. The signal enhancement results from the increase in plasma temperature and collision mechanism. The energy utilization efficiency of the reheating laser is higher than that in conventional orthogonal DP-LIBS when the reheating laser points to the surface of a solid aluminum target. The additional particles from the solid target are ablated by the reheating laser. Under the assistance of the solid target, collisions during plasma interactions promote re-excitation and ionization of species, which can lead to a considerable signal enhancement. The proposed target-enhanced orthogonal DP-LIBS allows the use of low ablative laser pulse energy and can improve analytical sensitivity with microablation and high spatial resolution. Moreover, the proposed technique can drastically improve the signal intensity of orthogonal DP-LIBS, and it can further improve the analytical sensitivity of orthogonal DP-LIBS and deliver superior analytical results. The proposed target-enhanced orthogonal DP-LIBS can find applicability in elemental analysis of precious samples and small samples in fields such as jewelry identification, art, archaeology, and materials science.

**Key words** spectroscopy; laser-induced breakdown spectroscopy; laser plasma; orthogonal double-pulse; solid target; signal enhancement

**OCIS codes** 300.6365; 300.6210; 300.6360